Journal of Sciences, Islamic Republic of Iran 31(2): 137 - 146 (2020) http://jsciences.ut.ac.ir
University of Tehran, ISSN 1016-1104

DFT Study and NBO Analysis of Conformation Properties of 2,5,5-Trimethyl-1,3,2-Dioxaphosphinane 2-Selenide and Their Dithia and Diselena Analogous

N. Masnabadi*

Department of Chemistry, Roudehen Branch, Islamic Azad University, Roudehen, Islamic Republic of Iran

Received: 14 October 2019 / Revised: 24 January 2020 / Accepted: 5 April 2020

Abstract

The hybrid density functional theory (B3LYP) and ab initio molecular orbital (HF) based methods and Natural Bond Orbital (NBO) interpretation were used to analyze the conformational behaviors of 2,5,5-trimethyl-1,3,2-dioxaphosphinane 2-selenide (compound **1**), 2,5,5-trimethyl-1,3,2-dithiaphosphinane 2-selenide (compound **2**) and 2,5,5-trimethyl-1,3,2-diselena phosphinane 2-selenide (compound **3**). The results explained that the axial conformations had a preference of compounds **1-3**. The relative energies ΔE_0 and Gibbs free energy difference values $(\Delta G_{eq\text{-}ax})$ between the ax and eq-conformations were calculated and showed the decrease from compound **1** to **3**. Stereo electronic effect (*SE*) for **1** to **3** has been calculated by the NBO analysis. Therefore, in this study, other factors such as stereo electronic effects, electrostatic and steric interactions of compounds **1** to **3** conformational behavior have been evaluated. One examined whether the stereo electronic effect is the only factor affecting the conformational behavior or not? The electronic properties such as the HOMO and LUMO energies were also determined to investigate the reactive sites of the compounds. Structural-relative activities of compounds are also evaluated.

Keywords: NBO; Stereo electronic interaction; Electronic properties; Dioxaphosphinane 2-selenide.

Introduction

Organophosphorus compounds have been widely used for agriculture for crop protection and pest control, over one hundred of them have been marketed for these purposes [1]. These compounds possess enzyme inhibition properties and as a result they can provide antibacterial and anticancer drugs [2-5]. Several studies of the conformation and structure of 1, 3, 2-dioxaphosphorinanes have been reported. These researches contain conformational analysis of 1,3,2-dioxaphosphorinane derivatives by ^{1}H, ^{13}C and ^{31}P NMR, X-ray, IR and also solid-state NMR studies [6], crystal and molecular structure determination of *cis*- and *trans*-2-morpholino-2-thioxo-4-methyl-1,3,2-dioxaphosphorinane and the 2-oxo analogue [7]. The isomer of 2-seleno-1,3,2-dioxaphosphorinane was virtually one chair conformer with equatorial 4-methyl and benzyl groups. A considerable population of the conformer with axial 4-methyl and seleno groups was indicated for this compound by NMR studies (in $CDCl_3$) [8].

The stabilization energies (*SEs*) related to electronic

* Corresponding author: Tel: +989124493793; Fax: +9866424314; Email: Masnabadi@riau.ac.ir, masnabadi2009@gmail.com.

delocalization and their effects on the conformational possessions of compounds **1-3** were quantitatively studied by the NBO analysis (e.g. Figure 1, Table 1). Also, there is no released experimental or quantitative theoretical information about the stereo electronic interaction influences on the compounds **1-3**. The resonance energies are commensurate to $S^2/\Delta E$ where ΔE is the energy differences between the donor and

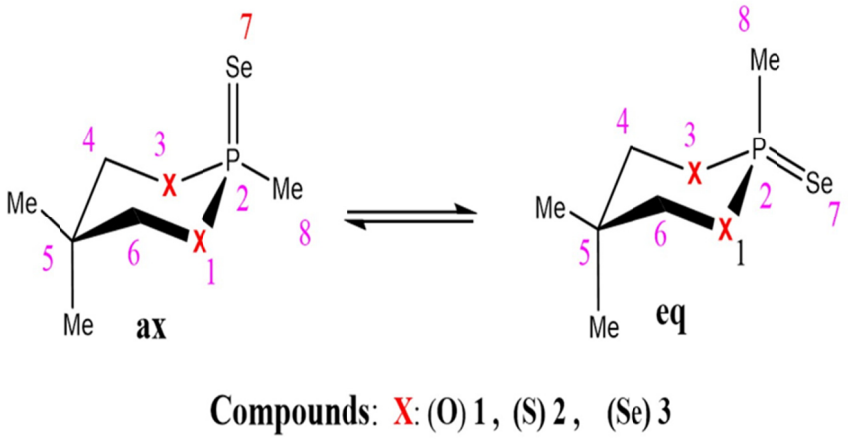

Figure 1. Representation of ax and eq-conformers of compounds **1-3.**

Table 1. The stereo electronic effect (*SE*) (in kcal mol^{-1}) associated with the Endo- and Exo-Anomeric orbital interactions, overlap matrix elements (*Sij*) (in a.u.), and Fock matrix elements (*Fij*) (in a.u.), in the compounds **1-3**, based on the geometries optimized at the B3LYP/6-311+G** level.

	Endo-Anomeric				
	$(n_{1X}\rightarrow\sigma^*_{P\text{-}Se})\times2$	$(n_{2X}\rightarrow\sigma^*_{P\text{-}Se})\times2$	$(n_{2X}\rightarrow\sigma^*_{P\text{-}C})\times2$	$(\sigma_{X\text{-}C6}\rightarrow\sigma^*_{P\text{-}C})\times2$	$(\sigma_{X\text{-}C6}\rightarrow\sigma^*_{P\text{-}Se})\times2$
1-ax					
SE	4.50	12.60	1.30	1.12	0.36
|Sij|	0.001	0.0926	0.1100	0.1694	0.0242
F_{ij}	0.036	0.048	0.017	0.022	0.012
2-ax	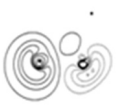	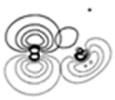			
SE	4.04	10.06	0.44	2.52	0.02
|Sij|	0.0680	0.1171	0.0285	0.1646	0.0118
F_{ij}	0.035	0.037	0.009	0.028	0.003
3-ax		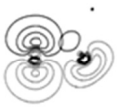	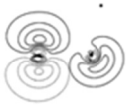		
SE	3.98	8.20	0.32	2.78	0.02
|Sij|	0.0598	0.1123	0.0280	0.1604	0.0221
F_{ij}	0.037	0.032	0.007	0.028	0.002

Table 1. Ctd

	Endo-Anomeric				
	($n_{1X}\rightarrow\sigma^*_{P\text{-}Se}$)×2	($n_{2X}\rightarrow\sigma^*_{P\text{-}Se}$)×2	($n_{2X}\rightarrow\sigma^*_{P\text{-}C}$)×2	($\sigma_{X\text{-}C6}\rightarrow\sigma^*_{P\text{-}C}$)×2	($\sigma_{X\text{-}C6}\rightarrow\sigma^*_{P\text{-}Se}$)×2
1-eq	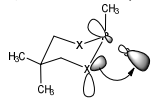	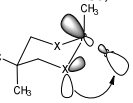	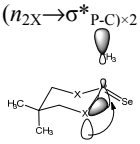	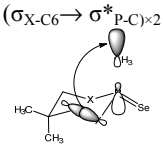	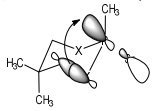
SE	0.94	1.34	13.08	0.00	2.50
|Sij|	0.0633	0.0482	0.1985	0.0057	0.1468
F_{ij}	0.016	0.016	0.053	0.002	0.031
2-eq					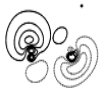
SE	0.12	0.34	10.18	0.18	3.76
|Sij|	0.0163	0.0243	0.1744	0.0361	0.1252
F_{ij}	0.006	0.007	0.041	0.007	0.032
3-eq	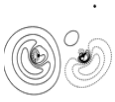	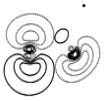	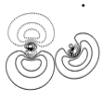		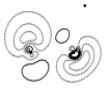
SE	0.50	0.36	8.54	0.16	3.94
|Sij|	0.0099	0.0267	0.1689	0.0400	0.1131
F_{ij}	0.013	0.007	0.037	0.007	0.032
			Exo-Anomeric		
	($n_{1Se}\rightarrow\sigma^*_{P\text{-}X}$)×2	($n_{1Se}\rightarrow\sigma^*_{P\text{-}C8}$)×2		($n_{1Se}\rightarrow\sigma^*_{P\text{-}X}$)×2	($n_{1Se}\rightarrow\sigma^*_{P\text{-}C8}$)×2
1-ax	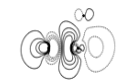		1-eq		
SE	1.80	2.82	*SE*	2.04	2.42
|Sij|	0.0389	0.0464	*|Sij|*	0.0674	0.0773
F_{ij}	0.027	0.033	*F_{ij}*	0.031	0.031
2-ax	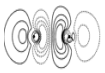		2-eq		
SE	2.82	3.20	*SE*	2.60	2.56
|Sij|	0.0608	0.0756	*|Sij|*	0.0716	0.0759
F_{ij}	0.032	0.036	*F_{ij}*	0.031	0.032
3-ax	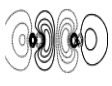		3-eq	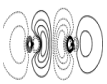	
SE	3.14	3.32	*SE*	2.86	2.64
|Sij|	0.0624	0.0767	*|Sij|*	0.0701	0.0736
F_{ij}	0.033	0.037	*F_{ij}*	0.032	0.033

acceptor orbitals and *S* is the orbital overlap. The *SE* associated *i*→*j* delocalization is explicitly estimated by following Eq. 1:

$$SE=-n_\sigma \frac{<\sigma|F|\sigma^*>^2}{\in_{\sigma^*}-\in_\sigma}=-n_\sigma \frac{F_{ij}^2}{\Delta E} \qquad \text{(Eq.1)}$$

Where $\mathcal{E}_\sigma$ and $\mathcal{E}_{\sigma^*}$ are the energies of σ and σ^* NBOs, $<\sigma/F/\sigma^*>$ or F_{ij} is the Fock matrix element between the *i*

and *j* NBO orbitals and σ^* is the population of the donor *S* orbital. Comprehensive explanations of the NBO calculations are accessible in the papers [9-17]. In this work, the conformational behavior of compounds **1-3** using NBO and HOMO/LUMO analysis, the *SE*, electrostatic interactions, structural and chemical parameters and *MEP* surfaces by B3LYP in 6-311+G** level were studied.

Materials and Methods

All the structures were totally optimized by the Gaussian 03 package at HF and B3LYP methods (with 6-311+G** basis set) [18]. After that, the B3LYP/6-311+G** level for the ax and eq-conformer were used by the NBO5.G program through the PC-GAMESS interface for achieving the NBO analysis [19, 20]. The *SE*s associated with Endo-Anomeric ($n_{1X}\rightarrow\sigma^*_{P\text{-}Se}$, $n_{2X}\rightarrow\sigma^*_{P\text{-}Se}$, $n_{2X}\rightarrow\sigma^*_{P\text{-}C}$, $\sigma_{X\text{-}C6}\rightarrow\sigma^*_{P\text{-}C}$ and $\sigma_{X\text{-}C6}\rightarrow\sigma^*_{P\text{-}Se}$) and Exo-Anomeric ($n_{1Se}\rightarrow\sigma^*_{P\text{-}X}$ and $n_{1Se}\rightarrow\sigma^*_{P\text{-}C8}$) electronic delocalization was computed using the NBO analysis (Table 1) [19]. The NBO analysis was used to study the electronical structures of the compounds models. The energies of hyper conjugative interactions, *Sij* and *Fij* matrix elements related to the orbital interactions, the hybridization and energies of donor and acceptor orbitals were estimated by using the NBO 5.0 program [19, 14, 20].

Results and Discussion

Conformational Preferences

The chair conformers of compounds **1-3** are more stable than their related twist-boat ones according to the HF and B3LYP methods with fully geometry optimization. The B3LYP/6-311+G**//B3LYP/6-311+G** and HF/6-311+G**//HF/6-311+G** computed zero-point energies *ZPE*, total energies E_0 and relative energies ΔE_0 (in kcal.mol^{-1}), for the maximum and minimum geometrical energeis of compounds **1-3** are shown in (Table 2). The total energies (E_0) of all ax-conformers are lower than the corresponding eq-conformers. Based on the results, the ax-conformers of compounds **1-3** have priority and the calculated (ΔE_{eq-ax}) amounts are shown in (Table 2). Also, The value of the thermodynamic functions H, S, G and the ΔG, ΔS and ΔH parameters are shown in (Table 3). The calculated ΔS values are relatively small, so that the calculated ΔH and ΔG parameters are close to the ΔE_0 values.

According to the results of $\Delta G_{eq\text{-}ax}$ values are shown in Table 3 the conformation stability of the axial relative to the equatorial counterpart change by changing the heteroatom in the ring. It means that ax-conformer

Table 2. Calculated total energies (E_0) (in hartree), zero-point energies (*ZPE*) and relative energies (ΔE_0) (in kcal mol^{-1}), for the energy-minimum and energy maximum geometries of compounds **1-3**.

	B3LYP /6-311+G**// B3LYP /6-311+G**				HF/6-311+G**//HF/6-311+G**			
Conformer	**ZPE**	**E_{el}**	**E_0**	**ΔE_0[a]**	**ZPE**	**E_{el}**	**E_0**	**ΔE_0[a]**
1-eq	0.189279	-3129.8244	-3129.635141	3.80	0.202708	-3125.205	-3125.016178	4.35
1-ax	0.189867	-3129.8311	-3129.641198	0.00	0.203077	-3125.2130	-3125.023111	0.00
2-eq	0.183607	-3775.7683	-3775.584691	2.02	0.196208	-3770.4962	-3770.312576	1.91
2-ax	0.183828	-3775.7717	-3775.587917	0.00	0.196346	-3770.4994	-3770.315625	0.00
3-eq	0.181233	-7782.4430	-7782.261767	0.77	0.193696	-7775.0219	-7774.840722	0.36
3-ax	0.181507	-7782.4445	-7782.262987	0.00	0.193811	-7775.0228	-7774.841298	0.00

[a] Relative to the ground state

Table 3. Thermodynamic Properties [ΔH, ΔG (in kcal mol^{-1}) and ΔS (in cal mol^{-1}K^{-1})] at 25ºC and 1 atm pressure for the axial and equatorial conformations of compounds **1-3**.

Conformer	B3LYP/6-311+G**//B3LYP/6-311+G**			HF/6-311+G**//HF/6-311+G**		
	ΔH^a (Hartree)	**ΔS^a**	**ΔG^a**	**ΔH^a**	**ΔS^a**	ΔG^a
1-eq	4.27	0.83	4.02	4.61	0.62	**4.43**
1-ax	0.00	0.00	0.00	0.00	0.00	**0.00**
2-eq	2.16	-0.01	2.19	2.10	0.07	**2.08**
2-ax	0.00	0.00	0.00	0.00	0.00	**0.00**
3-eq	0.96	0.40	0.84	0.62	0.06	**0.60**
3-ax	0.00	0.00	0.00	0.00	0.00	**0.00**

[a] Relative to the ground state

Table 4. Calculated dipole moment of compounds **1-3** at B3LYP/6-311+G** level

Compounds	**1-ax**	**1-eq**	**2-ax**	**2-eq**	**3-ax**	**3-eq**
μ (Deby)	4.21	6.54	3.48	6.64	3.41	6.45
Δμ(eq-ax)	2.33		3.16		3.04	

Table 5. The NBO calculated non-bonding and anti-bonding orbital energies, based on the calculated geometries using B3LYP/6-311+G** level of theory, for the axial and equatorial conformations of the chair and boat forms of compounds **1-3.**

	1		**2**		**3**	
Energies (a.u.)	**eq**	**ax**	**eq**	**ax**	**eq**	**ax**
$\mathbf{n_1X}$	-0.57277	-0.59931	-0.66838	-0.67772	-0.74790	-0.75776
$\mathbf{n_2X}$	-0.34227	-0.33916	-0.26095	-0.25686	-0.24541	-0.24012
$\mathbf{n_1Se}$	-0.76318	-0.76746	-0.80185	-0.80671	-0.81036	-0.81448
σ_{X-C6}	-0.84490	-0.83236	-0.60613	-0.60135	-0.55307	-0.54903
σ^*_{P-X}	0.37446	0.15481	0.02301	0.01904	-0.00545	-0.01009
σ^*_{P-Se}	0.11951	0.10904	0.08557	0.07850	0.08417	0.07928
σ^*_{P-C}	0.17572	0.18547	0.14080	0.14825	0.13915	0.14452
$\Delta E_{orbital}$ **(a.u.)**						
$\Delta E(\sigma^*_{P-Se} - n_{1X})$	0.69228	0.70835	0.75395	0.75622	0.83207	0.83704
$\Delta E (\sigma^*_{P-Se} - n_{2X})$	0.46178	0.4482	0.34652	0.33536	0.32958	0.3194
$\Delta E (\sigma^*_{P-C8} - n_{2X})$	0.51799	0.52463	0.40175	0.40511	0.38456	0.38464
$\Delta E (\sigma^*_{P-C8} - \sigma_{X-C6})$	1.02062	1.01783	0.74693	0.7496	0.69222	0.69355
$\Delta E (\sigma^*_{P-Se} - \sigma_{X-C6})$	0.96441	0.9414	0.6917	0.67985	0.63724	0.62831
$\Delta E (\sigma^*_{P-X} - n_{1Se})$	1.13764	0.92227	0.82486	0.82575	0.80491	0.80439
$\Delta E (\sigma^*_{P-C8} - n_{1Se})$	0.9389	0.95293	0.94265	0.95496	0.94951	0.959

stability is declining from compounds **1** to **3**. When oxygen is in the ring as a heteroatom, the ax-conformer shows better stability compared to compounds **2** and **3**. The dipole moment of ax and eq-conformers of compounds **1-3** calculated by B3LYP/6-311+G** (Table 4). The results obtained from the values of the dipole moment show that $\mu_{ax}<\mu_{eq}$ (Table 4), that the placement of P=Se in an equatorial form causes the dipole moment of ax-conformer reduce relative to eq one. Because P=Se is a polar group and its axial or equatorial orientation can affect on the amount of dipole moment of compounds **1-3**. Using Van′t Hoff ratio method, Shagidullin have showed that the enthalpy difference between the axial and equatorial conformers of compound **1** in the liquid phase is 0.2 kcal mol^{-1} in favor of the axial form. Also, these results showed that the polarity of the **1**-ax conformer is less than the **1**-eq conformer [21]. Therefore, the results collected in Tables 1 and 4 are consistent with the data reported by Shagidullin and co-workers. According the calculated values of μ, the $\Delta\mu_{eq-ax}$ values were calculated for compounds **1-3** (Table 4).

According to the NBO analysis stabilization energy associated with electron transfer $n_{2X}\rightarrow\sigma^*_{P-C}$ in eq-conformers and electron transfer $n_{2X}\rightarrow\sigma^*_{P-Se}$ in ax-conformers have the highest energy values, because the lone pair (n_{2X}) placement with P-C anti-bonding orbital in eq-conformers of compounds **1-3** is in the form of antiperiplanar (*ap*). Also, due to the difference in energy levels between donor bonding and acceptor anti-bonding orbitals of these transfers we found that $\Delta E_{orb}[\sigma_{p-c} - n_{2X}]$ (in eq-conformer) and $\Delta E_{orb}[\sigma_{p-Se} - n_{2X}]$ (in ax-conformer) for compounds **1-3** have the lowest amount compared to other ΔE_{orb} of the other transformations (Table 5).

Two factors due to the high *SE* of these compounds, One of them is the orbital orientation which should be *ap*, the other one is the vicinity of donor-acceptor energy levels. Again, the orbital orientation (*ap*) for two transfers $\sigma_{X-C6}\rightarrow\sigma^*_{P-C8}$ and $\sigma_{X-C6}\rightarrow\sigma^*_{P-Se}$ in eq- and ax-conformers for compounds **1-3** could be studied. According to the results of the NBO, we found that these two electrons transfer that is due to the proper orientation between donor and acceptor orbitals, have a significant energy since donor and acceptor orbitals be as an *ap* form. The donor and acceptor orbitals in Synclinal arrangement (*SC*), does not have a significant energy any more (Figure 2). In a way that the values of electronic transfer energy ($\sigma_{X-C6}\rightarrow\sigma^*_{P-C8}$ and $\sigma_{X-C6}\rightarrow\sigma^*_{P-Se}$) in ax-conformers of compounds **1** to **3** are not significant.

Based on the results of the NBO, the ΔE_{orb} increase for $\sigma_{X-C6}\rightarrow\sigma^*_{P-C}$ in ax-conformers of compounds **1-3** and they are close together and are approximately the same as eq-conformers. In the other words, their resonance energy domain is in a range. The *SE* do not have a wide range of changes by changing the heteroatom in the ring in eq-conformers, but stabilization energy of electron

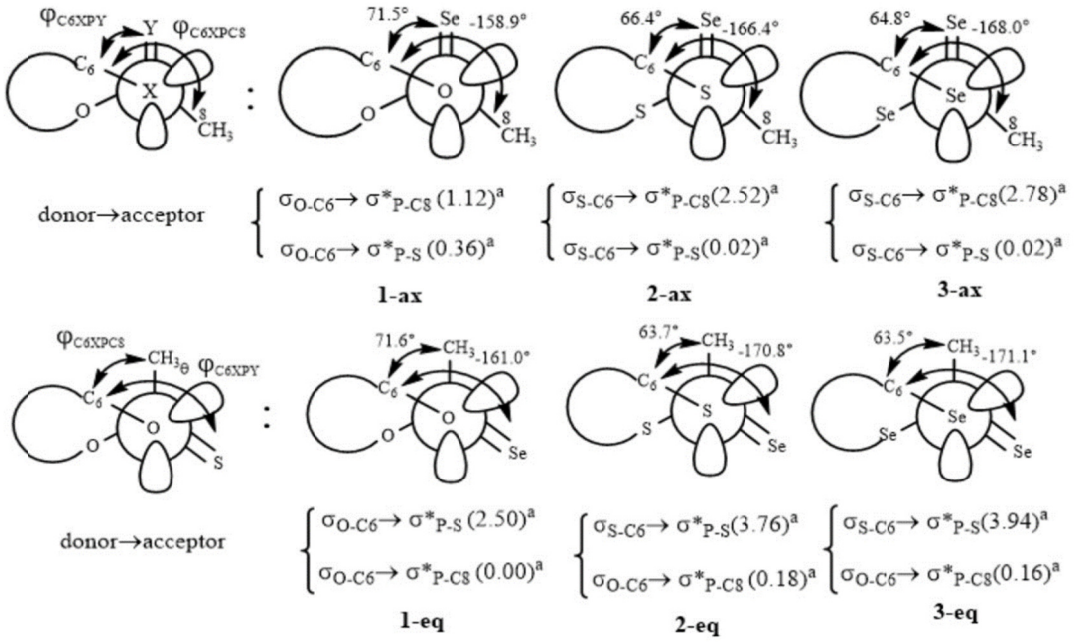

Figure 2. Presenting Newman Projections of conformers of compounds **1-3** and comparing the orientation of donor and acceptor orbitals them.

transfers changes tangible in ax-conformers (Figure 2).

Total electron transfers of compounds **1-3** in ax-conformers are more than eq-conformers. In other words, the *SE* of ax-conformers are more than eq-conformers. The results of the NBO analysis are in agreement with the values of thermodynamic properties. It means that the conformational behavior of studied compounds affected by stereo electron interactions.

According to the previous descriptions in this study, electron transfer the *SE* in eq-conformers with compounds **1-3** does not have a significant changing range. The orbital interaction between the donor and acceptor will be stronger when the difference in their energy level is low and vice versa. Overlap and Fock matrix elements for all the electron transfer interactions of compounds **1-3** using the NBO 5.0 are listed in Table 1. In order to qualitative study, the plots of electron transfers of compounds **1-3** by NBO View are shown in (Table 1).

Albeit the magnitude of the *SE* interactions depends on the rather complex interplay of geometric elements and inherent properties of interacting orbitals, the relative tendency in the energies of the *SE* interactions are easily explained by differences in the S_{ij} and F_{ij} factors related to these interactions. As stated by Eq.1, the energy of a *SE* interaction is straight compatible to the square of the respective the F_{ij} factor, and the correlation between these two qualities is brilliant. The analogous correlation should be used only in a qualitative sense and is less dependable with the overlap integral. The S_{ij} and the F_{ij} values for electron delocalization in the ax and eq-conformers of compound **1-3** calculated by the NBO. The enhancement of the X atom radius in these compounds could be played impressive role in the decline of the S_{ij} and the F_{ij} values, and can explain the decline of the *SE* values for compounds **1-3** (Table 1).

Bond order and structural parameters

Due to the presence of stereo electronic effects in ax and eq-conformers in compounds **1-3**, the bond orders P-Se, P-X, P-C_8 and X-C_6 have to change. Though this change in bond order is dependent on the stabilization energy of electron transfer.

As heteroatom changes in ring (O→S→Se), Calculated values of WBI (P-X) and WBI (P-Se) would have increasing and decreasing trend respectively. This decreasing is associated with increase of Exo-Anomeric effect (Table 6). It means that Exo-anomeric effect has less impact for justifying the reduction of values.

These results, it is remarkable that the bond lengths of P-X are increasing from compound **1** to **3** in ax and eq-conformers. Alteration range of P-X bond length is more tangible that that related to P-Se and P-C bond length. Considering the effects of Endo and Exo-anomeric, one can see again that increase of Exo-

anomeric effect has more influence on length increase of P-X bond than Endo-anomeric effect. It is remarkable when the angle of internal bond of X_1-P-X_3 is smaller than total angle of tetrahedral (109.48°), the phosphor atom will find fewer steric hindrance in comparison with linear phosphonate and the phosphor atom will have an available electrophilic center and increase the compound reactivity (Table 7). The bond angle of O-P-O (in **1**-ax) has the minimum amount among the bond angle of X_1-P-X_3 in other compounds. So, the phosphor atom can be a good center as an electrophile (Figure 3).

Therefore, this result is consistent with the real nature of the compound. If phosphor atom is attacked by a hypothetic nucleophile, the **1**-ax compound shows a better nucleophile reaction when compared with other compounds (**2** and **3**), because oxygen atom has a higher electronegative trait among sulfur and selenium (Table 7).

Table 6. Calculated Wiberg Bond Index (*WBI*) for the equatorial and axial conformations of compounds **1–3** at B3LYP/6-311+G** level.

Conformer	*WBI*			ΔWBI_{eq-ax}		
	P-Se	P-X	P-C_8	P-Se	P-X	P-C_8
1-eq	1.5117	0.6851	0.8652	0.0514	-0.002	-0.0353
1-ax	1.4603	0.6871	0.9005			
2-eq	1.3813	0.8815	0.8666	0.0186	0.015	-0.0322
2-ax	1.3627	0.8665	0.8988			
3-eq	1.3665	0.8664	0.8726	0.0076	0.0196	-0.0262
3-ax	1.3589	0.8468	0.8988			

Table 7. The B3LYP/6-311+G** calculated structural parameters for the equatorial and axial conformations of compounds **1-3.**

Compound	1		2		3	
Geometry	eq	ax	eq	ax	eq	ax
		Bond lengths (Å)				
r_{P-X1}=r_{P-X3}	1.635	1.637	2.138	2.144	2.290	2.302
r_{P-Se}	2.081	2.102	2.106	2.118	2.112	2.120
r_{P-C8}	1.826	1.806	1.856	1.828	1.839	1.833
		Bond angles (°)				
$\theta_{X1-P-X3}$	102.8	100.6	105.2	102.1	104.5	101.2
$\theta_{X1-P-Se}$=$\theta_{X3-P-Se}$	113.6	115.7	112.7	116.1	113.0	116.2
$\theta_{Se-P-C8}$	115.7	118.1	114.2	116.1	114.0	102.8
$\theta_{C6-X1-P}$= $\theta_{C4-X3-P}$	102.8	115.8	102.4	97.0	100.2	93.8
		Torsion angels (°)				
$\phi_{X1-P-X3-C4}$=$\phi_{X3-P-X1-C6}$	37.8	54.0	47.7	61.1	47.8	61.9
$\phi_{X1-C6-C5-C4}$=$\phi_{X3-C4-C5-C6}$	-57.7	-56.0	-71.0	-68.7	-73.3	-71.3
$\phi_{C5-C6-X1-P}$= $\phi_{C5-C4-X3-P}$	52.2	59.9	60.7	66.3	61.8	68.1
$\phi_{C6-X1-P-X3}$= $\phi_{C4-X3-P-X1}$	-37.8	-54.0	-47.7	-61.1	-47.8	-62.0
$\phi_{C6-X1-P-C8}$=$\phi_{C4-X3-P-C8}$	71.6	-159.0	63.7	-166.4	63.5	-168.0
$\phi_{C6-X1-P-Se}$=$\phi_{C4-X3-P-Se}$	-161.6	71.5	-107.8	66.4	-171.1	64.8

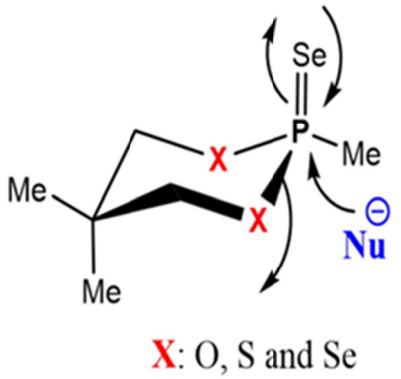

Figure 3. The phosphor atom can be a good center as an electrophile.

Because the changes in structural parameters in ax and eq-conformers explain with electrostatic and stereo electronic interactions. The results of structural parameters values show that by changing the heteroatom (O→S→Se) in the ring, increasing the radius of the atom in the ring. So, unfavorable 1,3-diaxial repulsion must be reduced and accordingly the steric effects decrease from compound **1** to **3**. But the results of thermodynamic properties show that steric effects have any role in justification the conformational behavior of compounds **1-3** and stereo electronic effects are dominant on steric effects in justification of conformational behavior.

HOMO/LUMO analysis

The lowest unoccupied molecular orbital (LUMO) and the highest occupied molecular orbital (HOMO) are the main parameters for quantum chemistry. The energy of the HOMO is immediately related to ionization potential, LUMO energy is immediately related to the electron affinity. In addition, the HOMO represents the ability to donate an electron and LUMO as an electron acceptor demonstrates the capability to obtain an electron. The HOMO/LUMO energy gap is the difference between HOMO and LUMO energy values and it is an important parameter for evaluating the molecular chemical stability. As a matter of fact, a large HOMO/LUMO gap alludes to high molecular stability in the concept of its lower activity in chemical reactions.

The energy value HOMO/LUMO for compounds **1-3** with the corresponding energy values of HOMO and LUMO frontier molecular orbitals are shown in (Figure 4). The important properties like chemical potential (μ), electronegativity (χ), global hardness (η), global softness (S), global electrophilicity index (ω) were calculated by using HOMO/LUMO analysis (Eq. 2). All

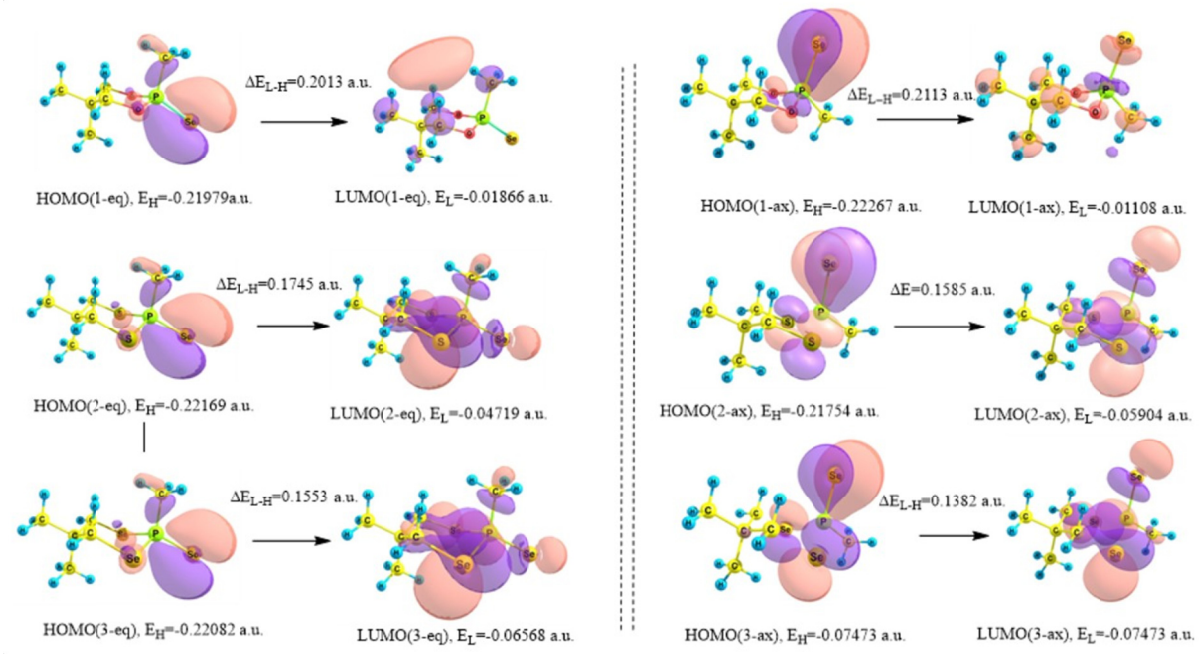

Figure 4. The HOMO and LUMO frontier molecular orbitals of axial and equatorial and comparison of HOMO/LUMO energy gaps in a.u. for compounds **1-3**.

Table 8. Calculated the chemical potential (μ), electronegativity (χ), global hardness (η), global softness (S), global electrophilicity index (ω) for axial and equatorial conformers of compounds **1-3** at B3LYP/6-311+G** level.

Compounds	μ	η	S	ω
1-ax	-0.116875	0.105795	4.726121272	0.064557709
1-eq	-0.119225	0.100565	4.971908716	0.070673697
2-ax	-0.13829	0.07925	6.309148265	0.120656934
2-eq	-0.13444	0.08725	5.730659026	0.103576582
3-ax	-0.143895	0.069165	7.229089858	0.149683879
3-eq	-0.14325	0.07757	6.445790899	0.132271255

these parameters for compounds **1-3** have been listed in Table and global reactivity described as [21-25] (Table 8).

Chemical potential (μ) = - χ, Electronegativity (χ) = -1/2 (E_L+E_H), Global hardness (η) = 1/2 (E_L- E_H), Global softness (S) = 1/(2η), Global electrophilicity (ω) = μ^2/(2η) (Eq. 2)

For more chemical hardness, the small HOMO/LUMO gap means a soft molecule and a large HOMO/LUMO gap means a hard molecule. The molecular stability can be related to the hardness, which means that the molecular with the least the HOMO/LUMO gap is more reactive the utility of the global electrophilicity index has been recently illustrated in perception of the toxicity of several pollutants in terms of their reactivity and site selectivity [26-27].

According to the results of HOMO/LUMO energy gap in compounds **1-3,** it seems that HOMO/LUMO gap amounts of ax-conformers are more than eq-conformers (Figure 4).

The results show that eq-conformers are more reactive than ax-conformers, in other words, ax-conformers are more stable than eq-conformers. Moreover, by changing the heteroatom in the ring the amount of $\Delta E_{L\text{-}H}$ is declining from compound **1** to **3** in ax and eq-conformers. This reduction in $\Delta E_{L\text{-}H}$ amounts shows that due to the change of heteroatom (O→S→Se) in the ring, increase the reactivity of compounds **1-3** and the stability of ax-conformers are declining from compound **1** to **3**. These facts are in agreement with the conformational behavior of compounds **1-3**, which has been studied in the conformational priority section (the $\Delta G_{eq\text{-}ax}$ values).

Conclusion

In this study, investigated the stability of corresponding to the equatorial and axial conformers of 2,5,5-trimethyl-1,3,2-dioxaphosphinane 2-selenide (compound **1**), 2,5,5-trimethyl-1,3,2-dithiaphosphinane 2-selenide (compound **2**) and 2,5,5-trimethyl-1,3,2-diselena phosphinane 2-selenide (compound **3**) were investigated by using the quantum mechanical methods. These compounds have been analyzed by means of DFT and HF techniques and natural bond orbital (NBO) interpretation. The axial chair conformation of compounds **1-3** are more stable than their corresponding equatorial conformations. Thermodynamic properties show that steric effects have any role in justification of the conformational behaviors of compounds **1-3** and stereoelectronic effects are dominant on steric effects in justification of conformational behaviors. Therefore, the greater stability of the concerned conformation was attributed to the stereo electronic effect. In other words, conformational preference is better explained in terms of stereo electronic effect rather than electrostatic and steric effects. The HOMO/LUMO energy gap and other related molecular properties are also calculated. According to the results of HOMO/LUMO energy gap in compounds **1-3** it seems that HOMO/LUMO gap amounts of ax-conformers are more than eq-conformers. Moreover, by changing the heteroatom in the ring the amount of $\Delta E_{L\text{-}H}$ is declining from compound **1** to **3** in ax and eq-conformers. This reduction in $\Delta E_{L\text{-}H}$ amounts show that due to the change of heteroatom (O→S→Se) in the ring, increasing the reactivity of compounds **1-3** and the stability of ax-conformers are declining from compound **1** to **3**. So, using above mentioned parameters, This work represents the conformational and chemical behaviors of mentioned compounds.

References

1. Bouchareb F., Hessainia S., Berredje M., Benbouzid H., Djebbar H., and Aouf N.E. Efficient method for the synthesis of diazaphospholidines: toxicological evaluation. *Am .J .Org .Chem*., **2**(1): 14-17 (2012).
2. Wu J., Sun W., Xia G., and Sun Y. A facile and highly efficient route to α-amino phosphonates via three-component reactions catalyzed by $Mg(ClO_4)_2$ or molecular iodine. *Org .Biomol .Chem*., **4** (9): 1663-1666 (2006).
3. Hiraga T., Williams P.J., Mundy G.R., and Yoneda T. The bisphosphonate ibandronate promotes apoptosis in MDA-MB-231 human breast cancer cells in bone metastases. *Cancer Res*., **61** (11): 4418-4424 (2001).
4. Bubenik M., Rej R., Nguyen-Ba N., Attardo G., Oullet F., and Chan L. Novel nucleotide phosphonate analogues with potent antitumor activity. *Bio. Med .Chem .Let*., **12** (21): 3063-3066 (2002).
5. Jankowski S., Marczak J., Olczak A., and Główka M.L. Stereochemistry of 1-hydroxyphosphonate–phosphate rearrangement. Retention of configu- ration at the phosphorus atom. *Tetra .Let*., **47** (20): 3341-3344 (2006).
6. Potrzebowski M.J., Bujacz G.D., Bujacz A., Olejniczak S., Napora P., Heliński J., Ciesielski W., and Gajda J. Study of molecular dynamics and the solid state phase transition mechanism for unsymmetrical thiopyrophosphate using X-ray diffraction, DFT calculations and NMR spectroscopy. *J .Phys .Chem .B*, **110** (2): 761-771 (2006).
7. Woźniak L. A., and Stec W. J. Oxidation in organophosphorus chemistry: Potassium peroxymonosulphate. *Tetra .Let*., **40** (13): 2637-2640, (1999).
8. Pir H., Günay N., Tamer Ö., Avcı D.**,** and Atalay Y. Assignment of cis-trans Theoretical investigation of 5-(2-Acetoxyethyl)-6-methylpyrimidin-2,4-dione: Conformational study, NBO and NLO analysis, molecular structure and NMR spectra. *Spect .Acta Part A: Mol .Bio . Spect*., **112**: 331-342 (2013).
9. Nori-Shargh D., Yahyaei H., and Boggs J.E.

Stereoelectronic interaction effects on the conformational properties of hydrogen peroxide and its analogues containing S and Se atoms: Ab initio, hybrid-DFT study and NBO analysis. *J .Mol .Graph .Mod*., **28** (8): 807-813 (2010).

10. Nori-Shargh D., and Boggs J.E. Complete basis set, hybrid□DFT study and NBO interpretations of conformational behaviors of trans-2,3 and trans-2,5-dihalo-1,4-dithianes. *J .Phys .Org .Chem*., **24** (3): 212-221 (2011).
11. Nori-Shargh D., Deyhimi F., Boggs J.E., Jameh-Bozorghi S., and Shakibazadeh R. DFT study and NBO analysis of the mutual interconversion of cumulene compounds. *J . Phys .Org .Chem.,* **20** (5): 355- 364 (2007).
12. Masnabadi N., Manesh A.T., and Azarakhshi F. Ab initio calculations of the conformational preferences of 1,3-Oxathiane *S*-Oxide and its analogs containing *S* and *SE* atoms-evidence for stereoelectronic interactions associated with the anomeric Effects. *Phosphorus, Sulfur, Silicon Relat. Elem.*, **188** (8): 1053-1063 (2013).
13. Azarakhshi F., khleghian M., and Farhadyar N. DFT study and NBO analysis of conformational properties of 2-substituted 2-Oxo-1,3,2-dioxaphosphorinanes and their dithia and diselena analogs. *Let. Org. Chem.*, **12** (7): 516-522 (2015).
14. Azarakhshi F., Nori-Shargh D., Masnabadi N., Yahyaei H., and Mousavi S.N. Conformational behaviors of 2-substituted cyclohexanone oximes: An ab initio, hybrid DFT study, and NBO interpretation. *Phosphorus, Sulfur, Silicon Relat. Elem.*, **187** (2): 276-293 (2012).
15. Süveges B.D., and Podlech J. Stereoelectronic effects in conformations of sulfide, sulfoxide, and sulfone α-carbanions. *Tetra.*, **71** (48): 9061-9066 (2015).
16. Alabugin I.V., and Zeidan T.A. Stereoelectronic effects and general trends in hyperconjugative acceptor ability of sigma bonds. *J. Am. Chem. Soc.*, **124** (12): 3175-3185 (2002).
17. Pagliero R.J., Lusvarghi S., Pierini A.B., Brun R., and Mazzieri M.R. Synthesis, stereoelectronic characterization and antiparasitic activity of new 1-benzenesulfonyl-2-methyl-1,2,3,4-tetrahydroquinolines. *Bioorg. Med. Chem.*, **18** (1): 142-150 (2010).
18. Weinhold F., Landis C.R., and Glendening E.D. What is NBO analysis and how is it useful? *Inter. Rev. Phys. Chem.*, **35** (3): 399-440 (2016).
19. Frisch M.J., Trucks G.W., Schlegel H.B., Scuseria G.E., Robb M.A., Cheeseman J.R., Montgomery J.A., Vreven T., Kudin K.N., Burant J.C., Millam J.M., Iyengar S.S., Tomasi J., Barone V., Mennucci B., Cossi M., Scalmani G., Rega N., Petersson G.A., Nakatsuji H., Hada M., Ehara M., Toyota K., Fukuda R., Hasegawa J., Ishida M., Nakajima T., Honda Y., Kitao O., Nakai H., Klene M., Li X., Knox J. E., Hratchian H.P., Cross J.B., Bakken V., Adamo C., Jaramillo J., Gomperts R., Stratmann R.E., Yazyev O., Austin A.J., Cammi R., Pomelli C., Ochterski J.W., Ayala P.Y., Morokuma K., Voth G.A., Salvador P., Dannenberg J.J., Zakrzewski V.G., Dapprich S., Daniels A.D., Strain M.C., Farkas O., Malick D.K., Rabuck A.D., Raghavachari K., Foresman J.B., Ortiz J.V., Cui Q., Baboul A.G., Clifford S., Cioslowski J., Stefanov B.B., Liu G., Liashenko A., Piskorz P., Komaromi I., Martin R.L., Fox D.J., Keith T., Laham A., Peng C.Y., Nanayakkara A., Challacombe M., Gill P M.W., Johnson B., Chen W., Wong M.W., Gonzalez C. and Pople J. A. **Gaussian 03, Revision B.03**, Gaussian, Inc.: Pittsburgh PA, (2003).
20. Glendening E.D., Badenhoop J.K., Reed A. E., Carpenter J.E., Bohmann J.A., Morales C.M. and Weinhold F. **NBO Version 5.G**., Theoretical chemistry institute, University of Wisconsin, Madison, WI, (2004).
21. Shagidullin R.R., Shakirov I.Kh., Musyakaeva R.Kh., Vandyukova I.I., and Nuretdinov I.A. Vibrational spectra and conformation of 2-methyl-2-seleno-1,3,2-dioxaphosphorinanes. *Russ. Chem. Bull.*, **30** (5): 916-918 (1981).
22. Winter A.H., and Falvey D.E. Vinyl Cations substituted with β π-donors have triplet ground states. *J. Am. Chem. Soc*., **132** (1): 215-222 (2010).
23. Haines B.E., Sarpong R., and Musaev D.G. Generality and strength of transition metal β-effects. *J. Am. Chem. Soc*., **140** (33): 10612-10618 (2018).
24. Sharma P.K., Petersen M., and Nielsen P. An α-d-configured bicyclic nucleoside restricted in an E-type conformation: synthesis and parallel RNA Recognition. *J. Org. Chem.,* **70** (13): 4918-4928 (2005).
25. Ayers P.W., and Parr R.G. Variational principles for describing chemical reactions: the fukui function and chemical hardness revisited. *J. Am. Chem. Soc*., **122** (9): 2010-2018 (2000).
26. Padmanabhan J., Parthasarathi R., Subramaniaan V., and Chattaraj P.K. Electrophilicity-based charge transfer descriptor. *J. Phys. Chem. A*, **111** (7): 1358-1361 (2007).
27. Sandford C., Fries L.R., Ball T.E., Minteer S.D., and Sigman M.S. Mechanistic studies into the oxidative addition of Co(I) complexes: combining electroanalytical techniques with parameterization. *J. Am. Chem. Soc*., **141** (47): 18877-18889 (2019).
28. Parthasarathi J., Padmanabhan J., Sarkar U., Maiti B., Subramanian V., and Chattaraj P.K. Toxicity analysis of aenzidine through chemical reactivity and selectivity profiles: A DFT approach. *Internet Electronic J. Mol. Des.*, **2** (12): 798-813 (2003).